Inorg. Chem. **2007**, *46*, 208–212

Synthesis, Crystal Structure, and Optical Properties of $LiGd_5P_2O_{13}$, a Layered Lithium Gadolinium Phosphate Containing One-Dimensional Li Chains

Jing Zhu, Wen-Dan Cheng,* Dong-Sheng Wu, Hao Zhang, Ya-Jing Gong, Hua-Nan Tong, and Dan Zhao

State Key Laboratory of Structural Chemistry, Fujian Institute of Research on the Structure of Matter, Yang Qiao Xi Road No. 155, Chinese Academy of Sciences, and the Graduate School of the Chinese Academy of Sciences, Fuzhou, Fujian 350002, People's Republic of China

Received August 14, 2006

A lithium gadolinium phosphate crystal, $LiGd_5P_2O_{13}$, has been synthesized by a high temperature solution reaction and solved by single-crystal X-ray diffraction data. The structure is monoclinic, space group *C*2/*m*, with unit cell parameters $a = 18.645(3)$, $b = 5.6257(5)$, $c = 12.014(2)$ Å, $\beta = 117.55(6)°$, $V = 1117.3(3)$ Å^3, and $Z = 4$. $LiGd_5P_2O_{13}$ presents a new structural type and is built up from $[Gd_5P_2O_{13}]^-$ layers and one-dimensional Li chains with an unusual Li–Li distance. The optical properties were investigated in terms of the absorption and emission spectra. Additionally, the calculations of band structure, density of states, dielectric constants, and refractive indexes were performed with the density functional threory method. The obtained results tend to support the experimental data.

Introduction

In the last couple of years stoichiometric alkali metal−rare earth phosphates have received much attention because they have shown a rich structural chemistry and interesting physical and chemical properties.[1−5] A lot of alkali metal−rare earth phosphates, such as $MLnP_2O_7$,[6−8] $MLn(PO_3)_4$,[9−13] and $M_3Ln(PO_4)_2$[14−17] (M = alkali metal, Ln = rare earth metal), have been synthesized and explored. The common basic structural unit of these materials is the PO_4 group, and the varied condensations of PO_4 groups may result in several structural families. Recently, we have reported $K_3Gd_5(PO_4)_6$ which presents a new structural family of the alkali metal−rare earth phosphate system with isolated PO_4 groups.[18] However, phosphate crystals with gadolinium have still been seldom reported, and the reports are mainly focused on the series of $MLn(PO_3)_4$[19−21] up to now. On the other hand, some phosphates involving lithium, such as $LiMPO_4$ (M = Fe, Co, or Ni),[22] exhibit excellent electrochemical properties with potential applications in lithium-ion batteries, and some alkaline metal gadolinium borates exhibit second harmonic

* To whom correspondence should be addressed. Fax: +86-591-371-4946. E-mail: cwd@fjirsm.ac.cn.

(1) Chinn, S. R.; Hong, H. Y. P. *Appl. Phys. Lett.* **1975**, *26*, 649.
(2) Otsuka, K.; Miyazawa, S.; Yamada, T.; Iwasaki, H.; Nakano, J. *J. Appl. Phys.* **1977**, *48*, 2099.
(3) Hong, H. Y. P. *Mater. Res. Bull.* **1975**, *10*, 1105.
(4) Ferid, M.; Horchani-Naifer, K. *Solid State Ionics* **2005**, *176*, 1949.
(5) Gavaldà, J. J.; Parreu, I.; Solé, R.; Solans, X.; Díaz, F.; Aguiló, M. *Chem. Mater.* **2005**, *17*, 6746.
(6) Ferid, M.; Horchani-Naifer, K. *Mater. Res. Bull.* **2004**, *39*, 2209.
(7) Ferid, M.; Horchani, K.; Amami, J. *Mater. Res. Bull.* **2004**, *39*, 1949.
(8) Khay, N.; Ennaciri, A. *J. Alloys Compd.* **2001**, *323*−*324*, 800.
(9) Zhu, J.; Cheng, W. D.; Wu, D. S.; Zhang, H.; Gong, Y. J.; Tong, H. N. *J. Solid State Chem.* **2006**, *179*, 597.
(10) Parreu, I.; Solé, R.; Gavaldà, J.; Massons, J.; Díaz, F.; Aguiló, M. *Chem. Mater.* **2003**, *15*, 5059.
(11) Zarkouna, E. B.; Driss, A. *Acta Crystallogr., Sect. E: Struct. Rep. Online* **2004**, *60*, i102.
(12) Yamada, T.; Otsuka, K.; Nakano, J. *J. Appl. Phys.* **1974**, *45*, 5096.
(13) Ferid, M.; Piriou, B.; Trabelsi-Ayedi, M. *J. Therm. Anal.* **1998**, *53*, 227.
(14) Hong, H. Y.-P.; Chinn, S. R. *Mater. Res. Bull.* **1976**, *11*, 421.
(15) Kloss, M.; Finke, B.; Schwarz, L.; Haberland, D. *J. Lumin.* **1997**, *72*−*74*, 684.
(16) Finke, B.; Schwarz, L.; Gürtler, P.; Krass, M.; Joppien, M.; Becker, J. *J. Lumin.* **1994**, *60*−*61*, 975.
(17) Kloss, M.; Schwarz, L.; Hölsä, J. P. K. *Acta Phys. Pol., A* **1999**, *95*, 343.
(18) Zhu, J.; Cheng, W. D.; Wu, D. S.; Zhang, H.; Gong, Y. J.; Tong, H. N.; Zhao, D. *Cryst. Growth Des.* **2006**, *6*, 1649.
(19) Amami, J.; Ferid, M.; Trabelsi-Ayedi, M. *Mater. Res. Bull.* **2005**, *40*, 2144.
(20) Parreu, I.; Solé, R.; Gavaldà, J.; Massons, J.; Díaz, F.; Aguiló, M. *Chem. Mater.* **2005**, *17*, 822.
(21) Naïli, H.; Mhiri, T. *Acta Crystallogr., Sect. E: Struct. Rep. Online* **2005**, *61*, i204.
(22) Ruffo, R.; Huggins, R. A.; Mari, C. M.; Piana, M.; Weppner, W. *Ionics* **2005**, *11*, 213.

10.1021/ic061536+ CCC: $37.00
Published on Web 12/13/2006

Table 1. Crystal Data and Structure Refinement for $LiGd_5P_2O_{13}$

formula	$LiGd_5P_2O_{13}$
formula weight (g mol^{-1})	1063.13
temperature (K)	293(2)
wavelength (Å)	0.710 73
crystal system	monoclinic
space group	*C*2/*m*
unit cell dimensions	$a = 18.645(3)$ Å $b = 5.6257(5)$ Å $c = 12.014(2)$ Å $\beta = 117.55(6)°$
volume, *Z*	1117.3(3) Å^3, 4
D_{calcd} (g cm^{-3})	6.320
μ (mm^{-1})	29.623
F(000)	1828
crystal size (mm)	0.32 × 0.03 × 0.02
θ range (deg)	3.46−27.46
limiting indexes	$-23 \le h \le 24$; $-7 \le k \le 7$; $-11 \le l \le 15$
reflections collected	4299
independent reflections	1397($R_{int} = 0.0492$)
refinement method	full-matrix least-squares on F^2
GOF	1.007
final *R* indexes [$I > 2\sigma(I)$]	$R_1 = 0.0382$, $wR_2 = 0.0932$
R indexes (all data)	$R_1 = 0.0460$, $wR_2 = 0.0984$
largest diff. peak and hole (e Å^{-3})	2.081 and −3.264

generation effects.[23,24] Accordingly, our research group is paying special attention to synthesizing and exploring new compounds that include the lithium and gadolinium elements.

In this paper, we will report the synthesis and structure of a new lithium gadolinium phosphate crystal, $LiGd_5P_2O_{13}$, which is the first example possessing a $[Gd_5P_2O_{13}]^-$ layered structure. The absorption and emission spectra of $LiGd_5P_2O_{13}$ will be measured. In addition, we will investigate its electronic properties and carry out the calculations of crystal energy band, density of states (DOS), dielectric constants, and refractive indexes of $LiGd_5P_2O_{13}$ by the density functional theory (DFT) method.

Experimental and Computational Procedures

Synthesis of $LiGd_5P_2O_{13}$. Single crystals of $LiGd_5P_2O_{13}$ were grown by using a high temperature solution reaction. Analytical reagents Gd_2O_3, Li_2CO_3, and $NH_4H_2PO_4$ were weighed in the molar ration of Li/Gd/P = 22:5:9, and the excess of Li_2CO_3 and $NH_4H_2PO_4$ acted as a flux. These starting materials were finely ground in an agate mortar to ensure the best homogeneity and reactivity, then placed in a platinum crucible, and heated at 573 K for 4 h in order to decompose Li_2CO_3 and $NH_4H_2PO_4$. Afterward, the mixture was reground and heated to 1323 K for 24 h. Finally, the temperature was cooled to 1073 K at a rate of 2 K/h and air-quenched to room temperature. A few colorless needle-shaped crystals were obtained from the melt of the mixture.

After crystal structure determination, a polycrystalline sample of $LiGd_5P_2O_{13}$ was synthesized by solid-state reactions of stoichiometric amounts (Li/Gd/P = 1:5:2) of analytical reagent Li_2CO_3, Gd_2O_3, and $NH_4H_2PO_4$. The pulverous mixture was allowed to react at 1253 K for 100 h with several intermediate grindings in an opening Pt crucible. The purity nature of the sample was confirmed by powder X-ray diffraction (XRD) studies using a Rigaku DMAX2500 diffractometer with Cu Kα radiation (step size of 0.05° and range $2\theta = 10-80°$). The powder XRD pattern of $LiGd_5P_2O_{13}$ is given in Supporting Information.

Single-Crystal Structure Determination. A single crystal of $LiGd_5P_2O_{13}$ with approximate dimensions of 0.32 × 0.03 × 0.02 mm^3 was selected for XRD determination. The diffraction data were collected on a Rigaku Mercury CCD diffractometer with graphite-monochromated Mo Kα radiation ($\lambda = 0.710\ 73$ Å) using the ω scan mode at the temperature of 293 K. The structure of the title compound was solved using direct methods and refined on F^2 by the full-matrix least-squares method with the SHELXL97 program package.[25] The position of the Gd atom was refined by the application of the direct method, and the remaining atoms were located in a succeeding difference Fourier synthesis. In order to confirm the chemical composition of the title compound, the $LiGd_5P_2O_{13}$ single crystal investigated on the diffractometer was analyzed by energy-dispersive X-ray spectrometry (EDX) using a JSM6700F scanning electron microscope. The obtained results are in good agreement with those obtained by the refinement of the crystal structure. No impurity elements have been detected, though the light element Li cannot be satisfactorily determined by EDX measurement. Further details on crystallographic studies and results of elemental analysis are given in Supporting Information.

Spectral Measurements. The absorption spectrum was recorded on a Lambda-35 UV/vis spectrophotometer in the wavelength range of 200−800 nm. The emission spectrum was measured on a FL/FS 900 time-resolved fluorescence spectrometer using a Xe lamp at room temperature.

Computational Descriptions. The crystallographic data of the solid-state compound $LiGd_5P_2O_{13}$ determined by XRD were used to calculate its energy band structure. The calculation of the energy band structure was carried out with DFT using a nonlocal gradient-corrected exchange-correlation functional (GGA-PBE) and performed with the CASTEP code,[26,27] which uses a plane wave basis set for the valence electrons and a norm-conserving pseudopotential[28] for the core electrons. The number of plane waves included in the basis was determined by a cutoff energy E_c of 450 eV. Pseudoatomic calculations were performed for O $2s^22p^4$, P $3s^23p^3$, Li $2s^1$, and Gd $4f^75s^25p^65d^16s^2$. The parameters used in the calculations and convergence criteria were set by the default values of the CASTEP code.[26] The calculations of linear optical properties were also made in this work. The imaginary part of the dielectric function, $\epsilon_2(\omega)$, can be thought of as detailing the real transitions between occupied and unoccupied electronic states. Since the dielectric constant describes a causal response, the real and imaginary parts are linked by a Kramers−Kronig transform.[29]

$$\epsilon_1(\omega) - 1 = \frac{2}{\pi} \mathrm{P} \int_0^\infty \frac{\omega' \epsilon_2(\omega')\, \mathrm{d}\omega'}{\omega'^2 - \omega^2} \text{ and } \epsilon_2(\omega) = -\frac{2\omega}{\pi} \mathrm{P} \int_0^\infty \frac{\epsilon_1(\omega')\, \mathrm{d}\omega'}{\omega'^2 - \omega^2}$$

where P means the principal value of the integral. This transform is used to obtain the real part of the dielectric function, $\epsilon_1(\omega)$.

(23) Zhang, Y.; Chen, X. L.; Liang, J. K.; Xu, T. *J. Alloys Compd.* **2002**, *333*, 72.
(24) Sasaki, T.; Mori, Y.; Yoshimura, M.; Yap, Y. K.; Kamimura, T. *Mater. Sci. Eng., R* **2000**, *30*, 1.
(25) Sheldrick, G. M. *SHELXTL-97: Program for Refining Crystal Structure;* University of Göttingen: Göttingen, Germany, 1997.
(26) Segall, M.; Linda, P.; Probert, M.; Pickard, C.; Hasnip, P.; Clark, S.; Payne, M. *Materials Studio CASTEP*, version 2.2; Accelrys, Inc.: San Diego, CA, 2002.
(27) Segall, M.; Linda, P.; Probert, M.; Pickard, C.; Hasnip, P.; Clark, S.; Payne, M. *J. Phys.: Condens. Matter* **2002**, *14*, 2717.
(28) Hamann, D. R.; Schluter, M.; Chiang, C. *Phys. Rev. Lett.* **1979**, *43*, 1494.
(29) Macdonald, J. R.; Brachman, M. K. *Rev. Mod. Phys.* **1956**, *28*, 383.

Table 2. Atomic Coordinates and Equivalent Isotropic Displacement Parameters for $LiGd_5P_2O_{13}$

atom	site	*x*	*y*	*z*	U_{eq}[a]
Gd1	4i	0.38972(4)	0.0000	0.43507(6)	0.0066(2)
Gd2	4i	0.19042(4)	0.0000	0.41173(6)	0.0086(2)
Gd3	4i	0.25916(4)	−0.5000	0.25605(6)	0.0083(2)
Gd4	4i	0.33493(4)	0.0000	0.10828(6)	0.0084(2)
Gd5	4i	0.52941(4)	−0.5000	0.66552(6)	0.0094(2)
P1	4i	0.1529(2)	0.0000	0.0682(4)	0.0140(8)
P2	4i	0.5568(2)	0.0000	0.2450(3)	0.0073(7)
O1	8j	0.5708(4)	−0.222(1)	0.3296(7)	0.017(2)
O2	8j	0.2025(4)	0.219(1)	0.0617(6)	0.012(2)
O3 (O3')	4i	0.168(2) (0.124(2))	0.0000	0.207(2) (0.162(3))	0.023(7) (0.02(1))
O4	4i	0.6145(6)	0.0000	0.120(1)	0.019(2)
O5	4h	0.5000	−0.257(2)	0.5000	0.008(2)
O6	8j	0.2868(3)	0.256(1)	0.4220(6)	0.011(2)
O7	8j	0.3626(4)	0.254(1)	0.2628(6)	0.008(1)
O8	4i	0.4687(6)	0.0000	0.139(1)	0.020(2)
O9	4i	0.0698(9)	0.0000	−0.032(1)	0.043(3)
Li	4g	0.0000	0.251(9)	0.0000	0.08(1)

[a] U_{eq} is defined as one-third of the trace of the orthogonalized U_{ij} tensor.

Table 3. Selected Bond Distances (Å) and Angles (deg) for $LiGd_5P_2O_{13}$

Gd1−O5	2 × 2.333(5)	Gd2−O6	2 × 2.262(6)
Gd1−O6	2 × 2.345(6)	Gd2−O6	2 × 2.296(6)
Gd1−O7	2 × 2.369(6)	Gd2−O1	2 × 2.522(7)
Gd3−O6	2 × 2.274(6)	Gd2−O3	2.30(2)
Gd3−O7	2 × 2.345(6)	Gd4−O7	2 × 2.206(6)
Gd3−O2	2 × 2.605(6)	Gd4−O2	2 × 2.416(6)
Gd3−O4	2.43(1)	Gd4−O2	2 × 2.578(6)
Gd5−O7	2 × 2.260(6)	Gd4−O8	2.35(1)
Gd5−O5	2 × 2.262(5)	Li−O9	2 × 2.07(4)
Gd5−O1	2 × 2.460(7)	Li−O8	2 × 2.45(3)
P1−O9	1.46(2)	P2−O4	1.50(1)
P1−O3	1.56(2)	P2−O8	1.55(1)
P1−O2	2 × 1.565(7)	P2−O1	2 × 1.552(7)
O9−P1−O3	118.6(12)	O4−P2−O8	110.0(6)
O9−P1−O2	2 × 112.8(4)	O4−P2−O1	2 × 110.5(4)
O3−P1−O2	103.6(6)	O8−P2−O1	2 × 109.4(4)
O3−P1−O2	103.6(6)	O1−P2−O1	106.8(6)
O2−P1−O2	103.9(5)		

Results and Discussion

Single-Crystal Structure. The structure of $LiGd_5P_2O_{13}$ belongs to the centrosymmetric space group *C*2/*m* with unit cell parameters $a = 18.645(3)$, $b = 5.6257(5)$, $c = 12.014(2)$ Å, $\beta = 117.55(6)°$, $V = 1117.3(3)$ Å^3, and $Z = 4$. Further details of the XRD structural analysis are given in Table 1. The atomic coordinates and thermal parameters are listed in Table 2. Selected bond lengths and angles are given in Table 3. It is found that the O3 atom displays positional disorder and occupies two equivalent positions (Table 2).

The three-dimensional (3D) framework of $LiGd_5P_2O_{13}$ consists of isolated PO_4 tetrahedra linked with Gd atoms distributed among them, and Li atoms are located in the infinite tunnels along the *b*-axis which are delimited by PO_4 tetrahedra and Gd polyhedra, as shown in Figure 1. There are two crystallographically different P atoms in isolated PO_4 tetrahedra. The P1 atom is surrounded by the O2, O3, and O9 atoms, whereas the P2 is coordinated by the O1, O4, and O8. All P−O distances vary in the range from 1.46(2) to 1.565(7) Å. The PO_4 tetrahedra are distorted, as it is seen from the values of the O−P−O angles from 103.6(6) to 118.6°(12) (Table 3). PO_4 tetrahedra are linked with Gd atoms by sharing O atoms to result in $[Gd_5P_2O_{13}]^-$ layers in the *ac* plane (Figure 2). Both Gd1 and Gd5 are six-coordinated, whereas Gd2, Gd3, and Gd4 are seven-coordinated. All Gd−O distances range from 2.206(6) to 2.605(6) Å (Table 3), as expected.[18,30] Gd3 polyhedra are greatly distorted. The Gd−Gd distances ranging from 3.570(1) to 4.009(1) Å are shorter than those in the $K_3Gd_5(PO_4)_6$ crystal we recently reported. Another distinct feature is that the coordination numbers of Gd atoms for $LiGd_5P_2O_{13}$ are six and seven, and those of Gd atoms for $K_3Gd_5(PO_4)_6$ are eight and nine. These $[Gd_5P_2O_{13}]^-$ layers share O atoms between them along the *b*-axis to form the 3D framework (Figure 2). The connection of PO_4 tetrahedra and Gd polyhedra delimits infinite tunnels along the *b*-axis in which the one-dimensional (1D) Li chains are located. As illustrated in Figure 3, the Li atom is coordinated by four O atoms with the Li−O distances ranging from 2.07(4) to 2.45(3) Å (Table 3). It is interesting to note that the mean Li−Li distance is 2.81 Å which is close to that of Li metal.[31] First, the unusual Li−Li distance in phosphates is found.

Band Structure and DOS. The energy band structure and DOS of $LiGd_5P_2O_{13}$ have been calculated with the DFT method. The spin polarization is properly taken into account because of the unpaired f-electron effect of the Gd^{3+} ion. Figure 4 illustrates the calculated band structure of $LiGd_5P_2O_{13}$. In order to assign these bands, total DOS (TDOS) and partial DOS (PDOS) are shown in Figure 5.

As shown in Figure 4, both the top of the valence bands (VBs) and the bottom of the conduction bands (CBs) exhibit slight dispersion. The lowest of the CBs is localized at the G point and has energy of 3.7032 eV. The highest energy of the VBs at the G point is −0.0253 eV, and at the M point is a value very close to that (0.0 eV). Accordingly, it is reasonable to consider $LiGd_5P_2O_{13}$ as an insulator with a direct band gap of around 3.73 eV. According to Figure 5, the O 2p states make main contributions to the top of the VBs near the Fermi level, and the Gd 6s states result in the VBs near −43.3 and −38.8 eV. The VBs near −5.36 eV are mostly formed by the Gd 4f states with the mixings of the O 2p and P 3p states, and the VBs near −7.58 eV are

(30) Rekik, W.; Naïli, H.; Mhiri, T. *Acta Crystallogr., Sect. C* **2004**, *60*, i50.
(31) Olinger, B.; Shaner, J. W. *Science* **1983**, *219*, 1071.

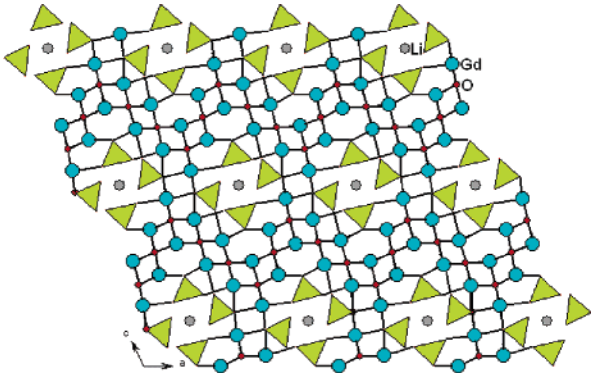

Figure 1. Projection of the structure of $LiGd_5P_2O_{13}$ along the *b*-axis (the Li−O bonds are omitted for clarity).

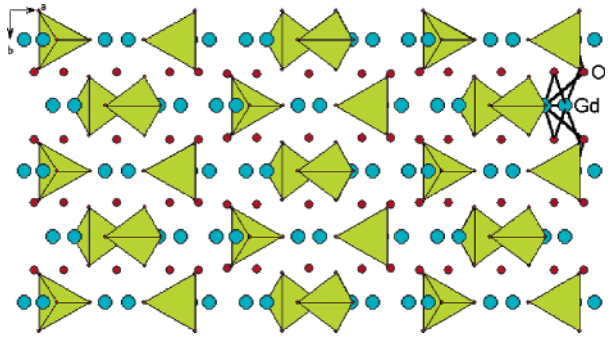

Figure 2. Projection of the structure of $LiGd_5P_2O_{13}$ along the *c*-axis (the Li atoms are omitted for clarity).

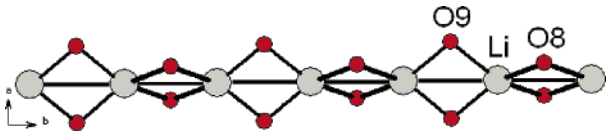

Figure 3. 1D Li chain along the *b*-axis.

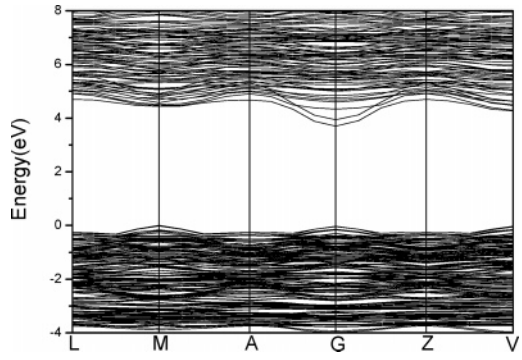

Figure 4. Calculated energy band structure of $LiGd_5P_2O_{13}$.

derived from the O 2p and P 3s states. The Gd 5p, O 2s, P 3s, and P 3p states give rise to the VBs from −22.1 to −13.0 eV. The bands from the bottom of the CBs to 12.0 eV result from the unoccupied Gd 5d and Gd 4f states with the mixing of the unoccupied P 3p and Li 2s states.

Optical Properties. Figure 6 illustrates the absorption and emission spectra of $LiGd_5P_2O_{13}$. The absorption edge is around 280 nm (4.44 eV), and the strong absorption peak appears at around 204 nm (6.09 eV; Figure 6a). The calculated band gap (3.73 eV) is smaller than the experimental one (4.44 eV). The reason for this situation is that the GGA cannot accurately describe the eigenvalues of the

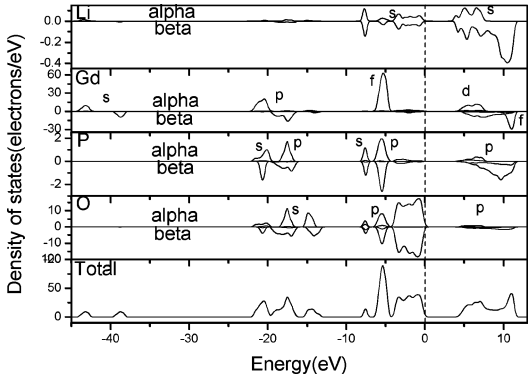

Figure 5. TDOS and PDOS of $LiGd_5P_2O_{13}$.

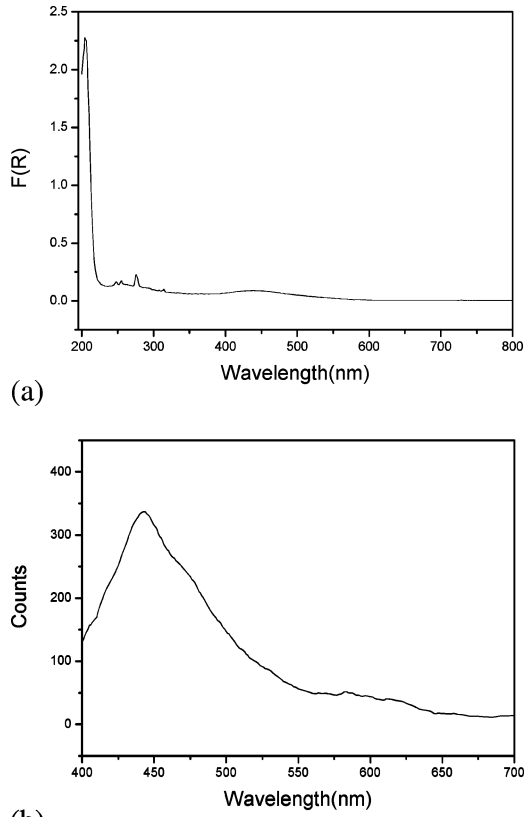

Figure 6. Absorption (a) and emission (b) spectra of $LiGd_5P_2O_{13}$.

electronic states, which causes quantitative underestimation of band gaps.[32] The emission spectrum of $LiGd_5P_2O_{13}$ exhibits a broad emission band at around 450 nm under the excitation of the wavelength at 357 nm (Figure 6b). The emitted energy of 2.76 eV (450 nm) is less than the optical absorption edge of 4.44 eV (280 nm). So, the emission band of $LiGd_5P_2O_{13}$ maybe originates from defects or excitons.

In addition, we examined the linear optical response properties of $LiGd_5P_2O_{13}$. We calculated the imaginary part $\epsilon_2(\omega)$ and the real part $\epsilon_1(\omega)$ of the frequency-dependent dielectric function without the DFT scissor operator approximation and with that of the shift energy of 0.71 eV, respectively. The refractive index is linked with the dielectric constant by the relation of $n^2(\omega) = \epsilon(\omega)$. The calculated

(32) Terki, R.; Bertrand, G.; Aourag, H. *Microelectron. Eng.* ***2005****, 81,* 514.

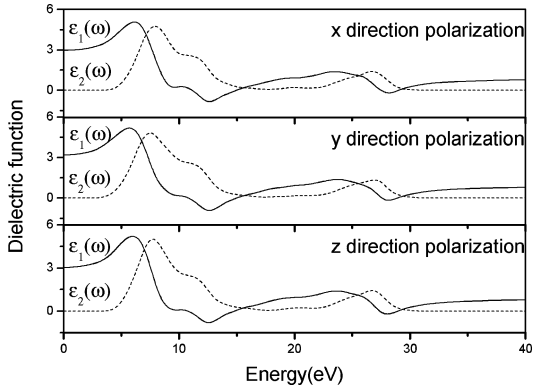

Figure 7. Calculated real and imaginary parts of dielectric functions of $LiGd_5P_2O_{13}$ in different polarization directions.

Table 4. Calculated Dielectric Constants of Static Case and Refractive Indexes at 1064 nm in Different Polarization Directions

scissor operator (eV)	$\epsilon_x(0)$	$\epsilon_y(0)$	$\epsilon_z(0)$	n_x	n_y	n_z
0	2.9740	3.1934	3.0442	1.7364	1.8019	1.7574
0.71	2.8240	3.0162	2.8857	1.6896	1.7479	1.7085

dielectric constants of static case $\epsilon(0)$ and the refractive indexes n at 1064 nm in x, y, and z directions are listed in Table 4. It is found that the calculated results with the shift energy of 0.71 eV are a little smaller than those without the DFT scissor operator approximation. Since the refractive indexes of $LiGd_5P_2O_{13}$ have not been measured and reported, we compare the calculated results with the observed refractive indexes of the other phosphate crystals which are generally ranging from 1.40 to 1.60.[33] Accordingly, our calculated refractive indexes derived from the dielectric constants maybe overestimate about 13%. Figure 7 displays calculated real and imaginary parts of dielectric functions of $LiGd_5P_2O_{13}$ in different polarization directions without the DFT scissor operator approximation. The part $\epsilon_2(\omega)$ can be used to describe the real transitions between the occupied and the unoccupied electronic states. There is a strong absorption peak around 7.70 eV which corresponds to that (6.09 eV) of the experimental spectra (Figure 6a). According to Figure 5, these peaks are assigned as the electronic transitions from the O 2p to the Gd 5d states. Comparing the calculated ultraviolet−visible absorption edge (4.26 eV) of the crystal with the experimental one (4.44 eV), we find that the calculated value is consistent with the experimental one.

(33) Dean, J. A., Ed. *Lange's Handbook of Chemistry*, 13th ed.; McGraw-Hill Book Company: New York, 1985.

Conclusions

In this work, a new lithium gadolinium phosphate crystal, $LiGd_5P_2O_{13}$, set up an interesting structural family of rare earth phosphates. It crystallizes in the monoclinic crystal system with space group $C2/m$ and is composed of $[Gd_5P_2O_{13}]^-$ layers and 1D Li chains with an unusual Li−Li distance. The broad emission band around 450 nm maybe originates from defects or excitons under the excitation of the wavelength at 357 nm. Both the experimental spectrum and the calculated band structure show that $LiGd_5P_2O_{13}$ possesses the insulating feature with a width of band gap. The top of the VBs originates from the O 2p states, and the bottom of the CBs results from the Gd 5d states. The absorption edge localized around 280 nm (4.44 eV) is assigned as the electron transitions from O 2p to Gd 5d states. Additionally, dielectric constants and refractive indexes of $LiGd_5P_2O_{13}$ are calculated. The calculated results are consistent with the experimental data. This study allows us to further synthesize and explore new alkali metal−rare earth mixed phosphates.

Acknowledgment. This investigation was based on work supported by the National Basic Research Program of China No2004CB720605, the National Natural Science Foundation of China under Project No. 20373073 and Project No. 90201015, the Science Foundation of the Fujian Province (No. E0210028), and the Foundation of State Key Laboratory of Structural Chemistry (No. 060007).

Supporting Information Available: X-ray crystallographic files (CIF) of $LiGd_5P_2O_{13}$, full results of elemental analysis for $LiGd_5P_2O_{13}$, and experimental and simulated powder XRD patterns of $LiGd_5P_2O_{13}$. This material is available free of charge via the Internet at http://pubs.acs.org.

IC061536+